Stability of the genetic structure of a wild wheat population across microhabitats over 36 years

Tal Dahan-Meir[1], Thomas James Ellis[2], Fabrizio Mafessoni[1], Hanan Sela[3,4], Jacob Manisterski[4], Naomi Avivi-Ragolsky[1], Amir Raz[1,5], Moshe Feldman[1], Yehoshua Anikster[4], Magnus Nordborg[2*], Avraham A. Levy[1*]

[1]Department of Plant and Environmental Sciences, Weizmann Institute of Science; Rehovot, Israel.

[2]Gregor Mendel Institute, Austrian Academy of Sciences, Vienna BioCenter; Vienna, Austria.

[3]Institute of Evolution, University of Haifa; Haifa, Israel.

[4]The Institute for Cereal Crops Improvement, Tel-Aviv University; Tel Aviv, Israel.

[5]Migal, Galilee Technology Center; Kiryat Shmona, Israel.

[*]Co-corresponding authors: [avi.levy@weizmann.ac.il; magnus.nordborg@gmi.oeaw.ac.at]

Abstract

Long-term genetic studies of wild populations are very scarce but are essential for connecting ecological and population genetics models, and are also necessary for understanding how climate change can affect biodiversity. We present a study of the wild ancestor of modern wheat, carried out over a 36-year period during which atmospheric CO_2 increased by 70 ppm and temperature by 1.5°C. We genotyped 832 individuals that had been collected along the same transects during the course of the experiment. To our surprise, very little changed. Genotypes were clustered into ecological microhabitats over scales of tens of metres, and this clustering was stable over the 36 generations of the study. Simulations indicate that neutral processes alone are unlikely to fully explain this stability, suggesting a role for fine-scale local adaptation. Our results provide a rare insight into the dynamics of a wild population at the scale of individuals.

Introduction

Climate change is a looming threat to plant biodiversity and food security (Hoffmann and Sgró, 2011; Pecl et al., 2017; Urban, 2015). This increases the importance of wild progenitors of crops because their genetic diversity is an immense reservoir of biotic and abiotic stress-resistance genes (Khoury et al., 2021). Long-term studies of progenitor species in their natural ecological niches can provide a better understanding of the likely impacts of climate change, and inform strategies for conservation of such resources *in-situ* as well as in gene banks (Wintle et al., 2019).

We examined the genetic diversity of a population of wild emmer wheat (*Triticum turgidum ssp. dicoccoides*) in Ammiad, Israel, which has been monitored for 36 years (Fig. 1A). During this period, local ambient temperatures increased by ~1.5 degrees Celsius (Fig. S1) and atmospheric CO_2 concentration increased by more than 20% (Fig. S2) (Keeling et al., 2001). This population was previously shown to be highly diverse in comparison with other populations, suggesting that it is located at the centre of distribution of the species (Felsenburg et al., 1991; Levy and Feldman, 1988). Wild emmer wheat is a self-pollinating, allotetraploid annual cereal (genome BBAA) that was domesticated about 10,000 years ago, during the Neolithic period (Avni et al., 2017; Nave et al., 2019; Salamini et al., 2002). It is the direct progenitor of durum wheat (*T. turgidum ssp. durum*) and the maternal donor of the A and B sub-genomes of bread wheat (*T. aestivum*, genome BBAADD). The population has been sampled at nine time points between 1984 and 2020. At each time point, seeds were sampled from plants at 100 marked locations along four transects traversing seven ecologically distinct microhabitats (Anikster and Noy-Meir, 1991) (Fig. 1A, Table S1, Movie S1). We genotyped 832 individuals using a genotyping-by-sequencing (GBS) protocol (Poland et al., 2012),

resulting in 5196 single-nucleotide-polymorphism (SNP) markers spread throughout the genome (Fig. S3).

Earlier spatio-temporal studies of wild plants involved shorter periods, as well as less comprehensive and less precise sampling (Franks et al., 2007; Fu et al., 2019; Horovitz and Feldman, 1991; Ozbek et al., 2007; Volis et al., 2004). Our dataset thus provides a unique resource for assessing genetic changes in a natural population in its natural habitat over many generations, and connects population genetic data with ecological sampling.

Results

As expected for a highly selfing species (The 1001 Genomes Consortium, 2016), the population is composed of genetically distinct groups of nearly identical, highly homozygous individuals clustered in space. Pairwise genetic identity follows a multimodal distribution that is characterised by pairs of plants that are either identical at almost all SNPs, or identical at 70% to 90% of SNPs (Fig. 1B). We unambiguously assigned all plants to distinct genotype groups (DGGs) of individuals that were identical at >98% of markers. This resulted in 118 DGGs over all nine time points, including 61 singletons (DGGs with a single member). The 10 largest DGGs encompass 65% of the samples, while the numbers of DGGs per year varied between 32 (2014) to 49 (1988; Table S2). Rarefaction curves indicate that the sampling scheme was sufficient to detect almost all of the DGGs present close to the transects (Fig. S4). These results provide a detailed picture of the genetic structure of the population through time and space.

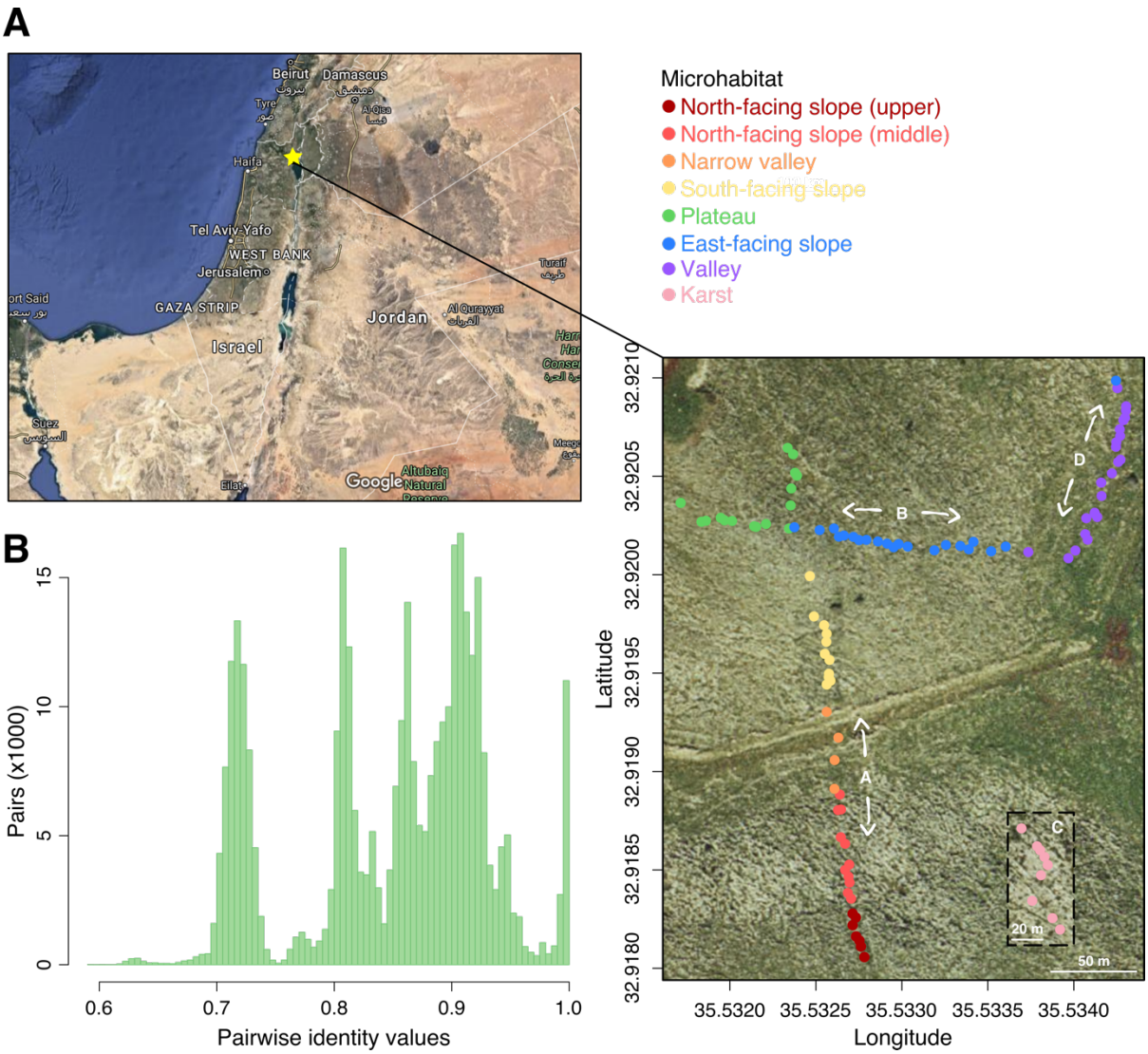

Fig. 1. Spatial structure of the Ammiad population. (A) Location of Ammiad near the lake of Galilee (star, top left and geographic coordinates, bottom right). Sampling points of transects A, B, C, D collected in the years 1984, 1988, 1992, 1996, 2002, 2014, 2016, 2018 and 2020. Sampling points are shown on-site for transects A, B, D, but transect C, shown in the dashed rectangle, is located ~500 meters north-west of A, B, D. Sampling points colours correspond to the different microhabitats labelled in the legend. Image of map on the right is from gov.map.co.il, map on the left from Google Maps. (B) Distribution of pairwise identity values between the plants in the collection.

The spatio-temporal distribution of DGGs shows that plants of the same DGG tend to cluster together in both space and time (Fig. 2 and Fig. S5). This clustering was also found in a principal component analysis (Fig. S6). Within years, the probability of belonging to the same DGG decays rapidly with distance (Fig. 3A), however, there is little evidence for isolation by distance beyond this (Fig. S7, S8). Overall, we find a striking concordance between DGGs and microhabitats, which were defined based on topographic and floristic data without knowledge of the genetic structure of the population (Noy-Meir et al., 1991b) (Fig. 2). For example, in transect A there is a sharp transition between DGGs of the upper and middle north-facing slope (Fig. 2A). Another example is the genotype at collection point A59 in a unique location under the shade of a *Ziziphus spina-christi* tree (Fig. 2A). In contrast, in transect D, where there is negligible microhabitat differentiation, plants of different DGGs were much more mixed (Fig. 2D). The spatial pattern was highly stable over the course of the experiment. In contrast to the rapid spatial decay, the probability of belonging to the same DGG decays only slowly over time (Fig. 3). For example, 33% of plants sampled in 1984 belonged to the same DGG as plants sampled at the same position in 2020. In conclusion, our results show a strong spatial structure, associated with microhabitat, which has remained stable for at least 36 years despite changes in climatic conditions.

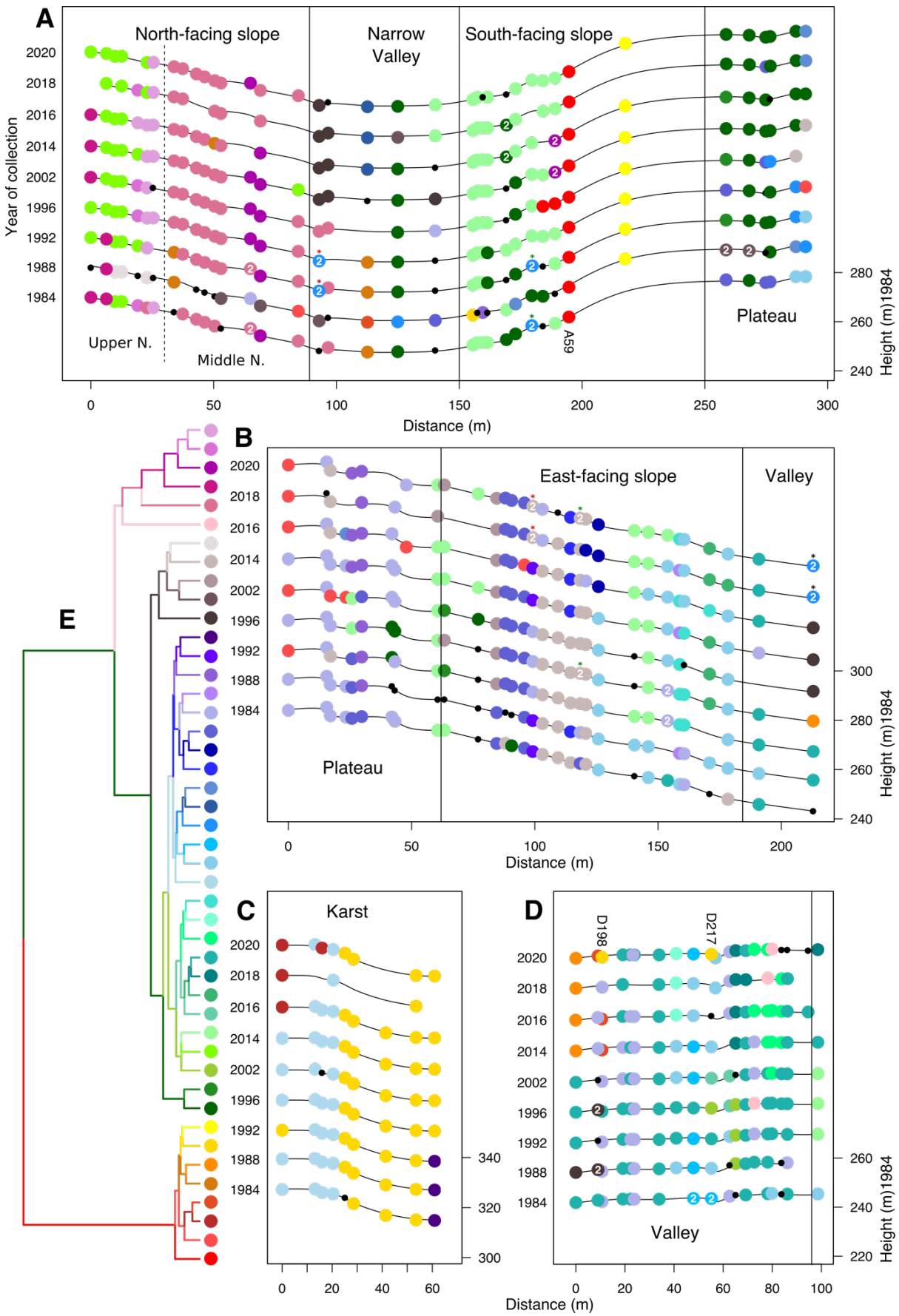
A
North-facing slope
Narrow Valley
South-facing slope
Year of collection
Upper N.
Middle N.
A59
Plateau
Height (m)1984
Distance (m)
B
East-facing slope
Valley
Plateau
C
Karst
D
D198
D217
Valley
E

121 **Fig. 2. Spatio-temporal distribution of genotypes.** (A-D) Distribution of samples coloured
122 by distinct genotype group (DGG) in transects A, B, C and D. Y-axes indicate year of
123 collection (left) and altitude for 1984 (right). Singleton samples are marked in small black
124 dots, while doubleton groups are marked with "2" in the middle with the colour of their
125 closest DGG. Doubleton groups that are closest to the same DGG were marked with coloured
126 asterisks. (E) Dendrogram of DGGs with ≥3 samples, hierarchically clustered by UPGMA.
127

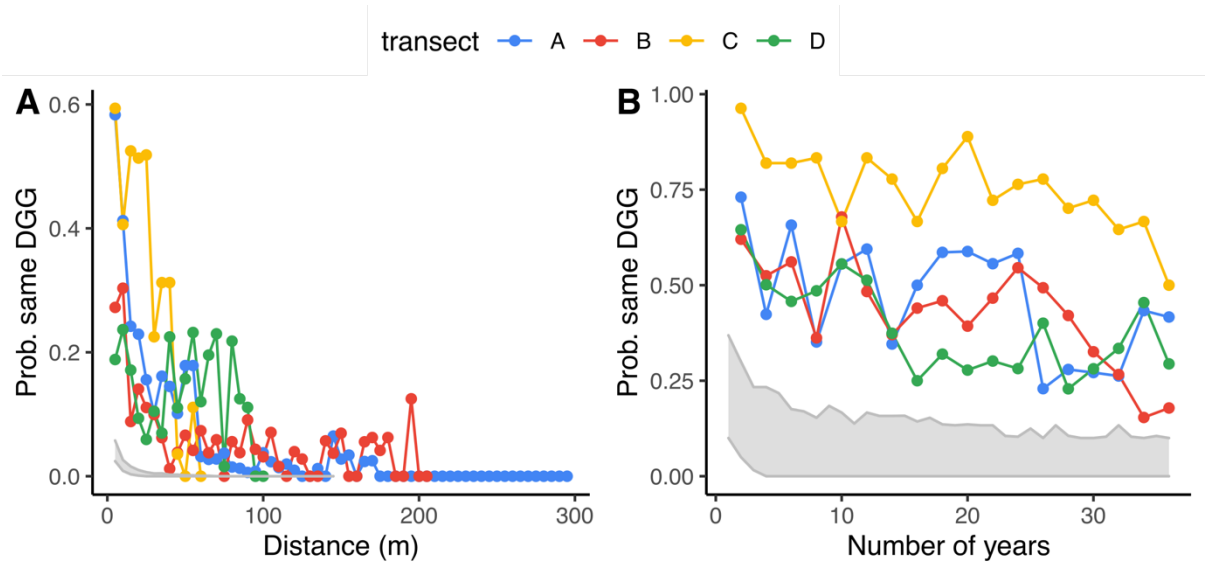

128

129 **Fig. 3. Spatial clustering and temporal stability at Ammiad.** Points show the probability
130 of observing genotypes of the same DGG at (A) pairs of sampling points in the same year at
131 increasing distances along each transect and (B) the same sampling point between pairs of
132 years. Grey regions indicate 95% confidence intervals over populations simulated under
133 conditions closest to empirical estimates (3 plants/m^2, mean seed dispersal of 1m, 0.5%
134 outcrossing per generation, 30% seeds germinating in the second year after dispersal). In A,
135 points show the average for sampling points in bins of 5m.
136

137 The observed patterns cannot be explained by simple chance. Across transects, pairs of the
138 same DGG were significantly more likely to be found in the same microhabitat in the observed

139 dataset than in 1000 permuted datasets where the order of microhabitats was randomly shuffled
140 (Fig. S9), or even when we control for distance and spatial autocorrelation, which could be
141 caused by limited dispersal, as shown via partial Mantel tests and Moran-spectral-
142 randomization Mantel statistics (MSR-Mantel) (Fig. S10). Similarly, population differentiation
143 measured by F_{st} was consistently higher between microhabitats than within, even when taking
144 distance into account (Fig. S11), and genetic distances are strongly correlated with
145 microhabitat. Furthermore, an analysis of molecular variance (AMOVA) showed that 28% of
146 the genetic variation between samples is explained by differences between microhabitats
147 (Table S3). In order to further test the hypothesis that the correspondence between the
148 population structure of Ammiad and microhabitats is shaped by processes other than limited
149 dispersal, we implemented an explicit demographic model that also incorporates self-
150 fertilization and limited seed dispersal. The question is whether these neutral demographic
151 processes - on their own - could generate the strong spatial clustering and temporal stability
152 observed at Ammiad.
153 To investigate this, we performed individual-based simulations of populations of plants in a
154 homogeneous environment, evolving by seed dispersal and outcrossing only. We ran
155 simulations using different values of outcrossing rate, plant density, seed dormancy and mean
156 seed dispersal distance that approximate a range of biologically realistic values. Empirical
157 values of outcrossing rates in wild wheat have been estimated to be approximately 0.5%
158 (Golenberg, 1988) with up to 30% of germinating seedlings coming from the seed bank
159 (Horovitz, 1998). Average plant density in the Ammiad population was measured in 1984 as
160 4 plants/m^2 (Noy-Meir et al., 1991a) and again in 2020 for transect A as 3.8 plants/m^2 (Fig.
161 S12, Table S4). We lack direct estimates of seed dispersal, but average gene flow, a composite
162 of seed and pollen dispersal, was estimated to be 1.25 m per year (Golenberg, 1987). Seed
163 dispersal occurs through a combination of gravity, ants, birds, grazing mammals and rodents,

enabling both short and long-distance dispersal. For example, the appearance of a DDG prominent in transect C (Fig. 2C, marked by yellow dot), in transect D in 2020 (Fig. 2D, locations D198, D217), more than 700 meters away, demonstrates that long distance movement occasionally occurs.

In simulations with the parameters we consider most likely (1 m mean seed dispersal, 0.5% outcrossing, density of 3 plants/m^2 and 30% seed dormancy) we find that neutral demographic processes alone could not account for the observed spatial clustering and temporal stability (Fig. 3), in line with other studies (Nevo, 2009). However, the simulation could produce results consistent with the data if we assumed extremely low plant densities ($\leq$1 plant/m^2) or rates of gene flow (outcrossing <0.5% when seed dispersal $\leq$ 1m) (Fig. S13-S16). Without better estimates of these parameters or direct fitness estimates from reciprocal transplant experiments, it is not possible to definitely reject a purely neutral explanation for the observed patterns. That said, the correspondence between DGGs and microhabitats is strong (Fig. 2 and Fig. S9-S11). Thus, the simulations indicate that it would be difficult to generate the observed patterns of stability over 36 years through neutral demographic processes alone.

Discussion

Studies of natural populations rarely have fine-scale geographic resolution, and almost never have temporal resolution beyond the duration of a PhD (Siepielski et al., 2009). Our study, spanning over 36 years of dense sampling, thus provides a unique dataset that could improve our understanding of gene flow and local adaptation - often modelled quite abstractly in population genetics - on an ecological scale.

187 Our analysis revealed that the collection of Ammiad population varies more in space than in
188 time. We found unexpectedly strong long-term genetic stability, demonstrating that gene flow
189 can be highly limited in a wild cereal despite its relatively wide distribution throughout the
190 fertile crescent. Remarkably, the stable genetic clusters observed in Ammiad matched
191 ecological microhabitats previously identified at the site, suggesting that natural selection, in
192 addition to limited dispersal, contributed to shaping population structure. Previous studies of
193 wild populations have demonstrated local adaptation (Abebe et al., 2015; Frachon et al., 2017;
194 Gardiner et al., 2018; Schemske, 1984; Sedlacek et al., 2016; Volis et al., 2016, 2015) over
195 large distances, but none at this spatial scale nor using long-term datasets. The possibility that
196 local adaptation occurs at such a fine spatial scale as in our study is particularly intriguing, and
197 invites experimental confirmation.
198
199 These results are relevant to conservation strategies as well as to the assessment of biodiversity
200 resilience under climate change. First, our study shows that *in-situ* conservation can be quite
201 effective in preserving diversity, without the need to frequently sample seeds and store them
202 in seed banks (*ex-situ*). Second, our results highlight that effective *in-situ* and *ex-*
203 *situ* conservation strategies of wild plants biodiversity, particularly for wild grasses and crop
204 progenitors such as wild emmer wheat, should consider habitat diversity as a potential reservoir
205 of adaptive diversity. In fact, our long-term study would not have been possible if the site had
206 not been declared a natural reserve for wild-wheat conservation by the Israel nature and parks
207 authority. Indeed, this population is fenced and undergoes moderate grazing. Unrestricted
208 grazing, or urbanization, as seen in other parts of the Levant can reduce and sometimes
209 eliminate wild grasses. The Ammiad reserve is relatively small (~10 hectares), but contains
210 much diversity. Establishing natural reserves of crop progenitors, partially protected from

211 anthropogenic activities, does not necessarily require large areas and is a feasible goal that is
212 critical for biodiversity conservation.
213
214 In conclusion, we provide evidence for strong genetic stability in a wild grass, most likely due
215 to a combination of local adaptation and limited dispersal. This stability is remarkable given
216 that, during the period of this study, temperatures and CO_2 levels increased significantly (Fig.
217 S1, S2). Yet only rather minor changes occurred in the population genetic structure, reflecting
218 the ability of wild plants to deal with changing environments and pointing to the robustness of
219 wild emmer wheat. Such robustness further demonstrates the importance of conservation of
220 wild relatives of crops in nature, as gene pools for breeding (Zsögön et al., 2021).
221
222 Archaeological excavations of a hunter-gatherers' site on the shore of Lake Galilee uncovered
223 an abundant wild emmer wheat, indicating that it has been present in the region of Ammiad for
224 at least 23,000 years (Snir et al., 2015). Since then, the Levant has undergone major climatic
225 changes, including several cycles of glaciation, warming and cooling (Zeder, 2011), pointing
226 to the robustness of wild emmer wheat. Nevertheless, temperatures and atmospheric CO_2
227 concentrations have never been as high as they are now during that period, therefore, it is
228 unclear to what extent additional changes in environmental conditions could occur before
229 negative consequences for population fitness became apparent.

230 Materials and Methods

231 Sample collection and DNA extraction

232 Wild wheat spikes were collected in four different linear transects every 3 to 5 meters from
233 sampling points marked with pegs and GPS coordinates (Table S1). Plants were assigned to a

234 sampling point when collected in successive years in a radius of ~ 1m from the peg. A single
235 seed was selected for each plant and DNA was extracted from young seedlings. Tissue was
236 collected and ground using mortar and pestle with the addition of Merck sea sand in liquid
237 nitrogen. DNA extraction was done using Macherey-Nagel NucleoSpin® Plant II extraction
238 kit, according to the manufacturer's protocol, eluting in 50 ul EB total. Concentrations and
239 DNA quality were estimated using a NanoDrop® ND-1000 Spectrophotometer.

240 **Genotyping by sequencing (GBS) and variant calling**

241 Plant genotyping was done according to the Genotyping-By-Sequencing method (Elshire et al.,
242 2011; Poland et al., 2012). Samples were sequenced using Illumina NextSeq 550 mid-output
243 150 base-pairs single-end kits. A reference sample, Zavitan accession (Avni et al., 2017), was
244 added to each run, undergoing the same plate GBS library preparation and sequencing. Samples
245 were divided by barcodes using a python 2.7 code. Mapping to the WEW_v2.0 genome
246 assembly (Zhu et al., 2019) was done using *bwa-mem* (Li, 2013). Conversion to binary
247 alignment map (BAM) format, filtering for uniquely mapped reads with minimum QUAL score
248 of 30, sorting and indexing was done using SAMtools (Li et al., 2009). Variant calling was
249 done in parallel running on all 845 (832 Ammiad samples and 13 Zavitan controls) samples
250 using GATK HaplotypeCaller 3.8(Poplin et al., 2018). Filtering for quality (>30), read depth
251 (>6), genotype quality (>15), maximum missing sites (10%) and no-indels was done using
252 VCFtools (Danecek et al., 2011). Filtering for up to 10% heterozygous plants per polymorphic
253 position was done using TASSEL5 (Bradbury et al., 2007). Filtered VCF was used for all
254 further analyses.

255 **Pairwise genetic identity**

256 Identity was measured using R code which calculates the pairwise identity values between all
257 samples, divided by the numbers of comparisons. The pipeline also includes the division of the

258 samples to distinct genotype groups (DGGs), done by setting a threshold of 98.1% identity,
259 which is the lowest threshold where no sample is assigned to two or more DGGs. and the
260 construction of the dendrogram describing the relatedness between the DGGs. Hierarchical
261 clustering was done in R by UPGMA. The 13 Zavitan reference samples added to each run
262 were grouped together with 99.4% identity. Heatmap of samples from 1984 was done using
263 *pheatmap* (https://cran.r-project.org/web/packages/pheatmap/index.html) with default
264 hierarchical clustering.

265 **Temperature and CO2 concentration data**

266 Data of daily minimum and maximum temperature from 1984 to 2020 were obtained from
267 Israel Meteorological Service at the Israel government portal (https://ims.data.gov.il/he/ims/2).
268 Data of weekly atmospheric CO2 concentrations were obtained from The Scripps Institution
269 of Oceanography UC San Diego (Keeling et al., 2001).

270 **Rarefaction, principal component and identity by distance analyses**

271 Rarefaction analysis was done using R, sampling backwards by the number of samples and
272 different genotypes, per year, 100 times and adjusting a polynomial to each sampling.
273
274 Principal component analysis was done on the .vcf file of the entire Ammiad collection using
275 *SNPRelate* R Package (Zheng et al., 2012). Identity by distance was correlated for each transect
276 separately. Pairwise Euclidean distances was calculated using the *distHaversine* function of
277 *Geosphere* R package (https://cran.rproject.org/web/packages/geosphere/index.html). Mantel
278 test with 1000 permutations was used to calculate correlation between the genetic identity and
279 the Euclidean distance matrices, using *mantel.test* in *Ape* R package (Paradis et al., 2004).

280 **Individual-based simulations**

281 To investigate whether neutral demographic processes could account for the observed spatial
282 clustering and temporal stability we performed individual-based simulations of populations of
283 plants evolving via seed dispersal and outcrossing only. Briefly, we allow populations to evolve
284 in a 2-dimensional continuous space, then draw a transect through the population and sample
285 plants close to 30 evenly spaced sampling points in the last 36 generations to replicate the
286 sampling procedure in the empirical dataset. An R package, *simmiad*, is provided to perform
287 these simulations (DOI:10.5281/zenodo.4762083).

288

289 Populations begin with N plants of a single genotype distributed randomly through a
290 homogeneous habitat with 1, 2, 3 or 5 plants/m^2. At each generation, N plants are sampled with
291 replication to produce N seeds. Wild emmer wheat has a two-year seed bank, so from
292 generation 3 onwards, seeds are drawn from the previous generation with probability p, and
293 from two generations previous with probability 1-p, for values of p of 0.5, 0.7, 0.9 or 1 .Since
294 we are only concerned with tracking unique genotypes, and information about seed dispersal
295 is in any case lacking model outcrossing as analogous to mutation; seeds are randomly assigned
296 as outcrossed with probabilities 0.25%, 0.5%, 1%, or 2%, in which case it is assigned a new
297 unique genotype. Offspring disperse from the mother in a random direction at a distance drawn
298 from an exponential distribution with a mean of 0.5, 0.75, 1 or 2m. To eliminate edge effects,
299 the habitat is modelled as a torus, such that if dispersal takes a seed over the edge of the habitat
300 it is reflected back to the opposite side. We allowed populations to evolve for 2000 generations
301 to ensure populations had reached equilibrium. We then drew a transect of 30 sampling points
302 5m apart through the middle of the population, and sampled the plant closest to each sampling
303 point in each of the final 36 generations of the simulations, replicating the sampling procedure

304 in the field. For each combination of plant densities, outcrossing rates, seed bank parameter *p*,
305 and seed dispersal distances we performed 100 replicate simulations.

306 **Microhabitat sorting and analysis**

307 We aimed to test the hypothesis that the population structure of Ammiad wild wheat reflects
308 that of microhabitats. We tested this using two different statistics and permutation schemes.
309 First, we tested whether plants in the same DGG tend to be confined to a single microhabitat
310 more than would be expected by chance using a procedure analogous to a permutation test. We
311 concatenated microhabitat and DGG labels across transects, and calculated how often pairs of
312 plants of the same DGG were located in the same microhabitat. We then shuffled the order of
313 microhabitats, whilst keeping labels of the same microhabitat together, and recalculated how
314 many pairs of plants of the same DGG were located in the same microhabitat after shuffling.
315 We repeated this shuffling procedure 1000 times, and compared the observed number of
316 matching pairs within the same microhabitat to the distribution of shuffled datasets. This
317 procedure randomises the relationship between the locations of DGGs and microhabitat
318 boundaries, but maintains the overall spatial structure of DGGs and microhabitats.
319 Second, we tested whether population differentiation, measured by F_{st}, is higher when
320 measured between plants occurring in different microhabitats than in the same microhabitat.
321 To this goal we subdivided plants into demes with a maximum distance between plants of 30m.
322 We then computed the pairwise Fst between demes using the R package *pegas* (Paradis, 2010).
323 To correct for the effects of isolation by distance and spatial structure we stratified comparisons
324 by distance, measured as the distance between the average locations of plants in the two demes.
325 We computed an analysis of molecular variance using the R package *pegas* (Paradis, 2010),
326 using plants sampled across all years and restricting the analysis only to genotypes present in

Ammiad. We included two factors, microhabitat and year of collection, with the latter nested within the former.

To account for spatial autocorrelation we first performed a partial Mantel test using the function *multi.mantel* from the R package *phytools*. Specifically, we considered as a response variable the pairwise genetic distances used to define DGGs. We tested for the effect of habitat, represented as a distance matrix with value "0" for plants found in the same microhabitat and "1" for plants found in two different microhabitats. In addition, we included in the test a matrix of time distances between the sampling of two plants (distance measured in years) and spatial distance, measured in metres and obtained from latitude and longitude using the function *earth.dist* from the R package fossil. We detected a significant effect of space and microhabitat (p-values <0.005 for both matrices) and a non-significant effect of time (p-value 0.863).

Note that Mantel and partial Mantel tests have severely been criticised for their inaccuracy in presence of high spatial autocorrelation (Crabot et al., 2019; Legendre et al., 2015). To account for these known biases, we used the approach proposed by (Crabot et al., 2019), which leverages a Moran spectral randomization procedure to generate random samples which maintain the same autocorrelation properties of the original dataset. To this goal, we used the R packages *sdpep* to process the spatial matrices and the *msr* function of the package *adespatial*. The distances above were transformed into Euclidean distances with function *cailliez* from the R package *adegenet*. Using this approach, we tested the effect of habitat on both DGGs and pairwise genetic distances, using 1000 randomizations. In both cases the effect of microhabitat was significant (p-value<0.05).

349 ## Data and code availability

350 Sequencing data generated in this study are available in the National Center for Biotechnology
351 Information (NCBI) Sequence Read Archive (SRA) under the accession number
352 PRJNA779576. All data processing and data analysis are publicly available on GitHub
353 (https://github.com/TalDM/Ammiad). An R package, *simmiad*, is provided to perform the
354 individual-based simulations (DOI:10.5281/zenodo.4762083).

355 ## Acknowledgements

356 We thank T. Azulay, T. Grinevich, C. Melamed-Bessudo, O. Gross, R. Epstein, O. Rudich, Z.
357 Meir and members from the Institute for Cereal Crops Improvement at Tel-Aviv University for
358 plant material collection and J. Müller for the drone movie. We also thank D. Filiault, K.
359 Swarts, S. Nowoshilow, N. De-Malach, R. Pisupati, R. Burns, Y. Voichek, P. Clauw, E.
360 Kosman and the Levy and Nordborg labs for fruitful discussions.

361 ## Author Contributions

362 T.D-M., M.F., Y.A. and A.A.L, conceived and designed the study. T.D-M. carried out the
363 molecular work, SNP calling and genetic analyses with input from T.J.E., F.M., M.N. and
364 A.A.L. T.J.E. performed the simulations and microhabitat sorting analyses with input from
365 T.D-M., M.N. and A.A.L. F.M. carried out the population differentiation analysis and the
366 MSR-Mantel tests. T.D-M., H.S., J.M., N.A-R., A.R., M.F., Y.A, and A.A.L carried out the
367 collection. T.D-M., T.J.E., F.M, M.N. and A.A.L wrote the manuscript. M.N. and A.A.L
368 supervised the project.

Funding

This work was supported by the Yeda-Sela Center and Sustainability and Alternative Energy Research Initiative of the Weizmann Institute of Science. T.D-M. acknowledges a European Molecular Biology Organization scientific exchange grant 8368.

Ethics declaration

The authors declare no competing interests.

Supporting Information

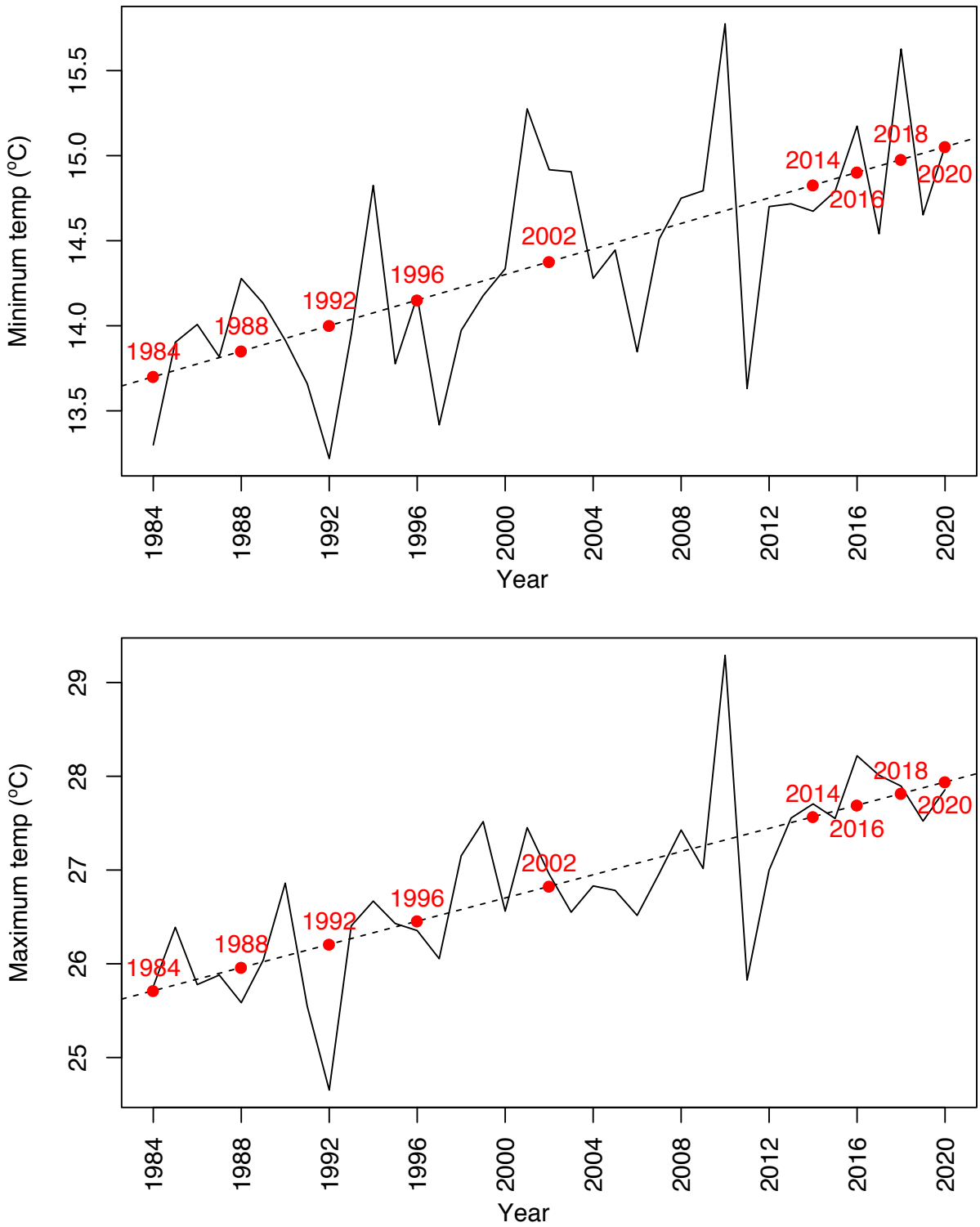

Fig. S1. **Average yearly minimum (A) and maximum (B) temperature measured in Ayelet Haschahar weather station from 1984 to 2020**. Collection years are marked in red on the linear model regression line.

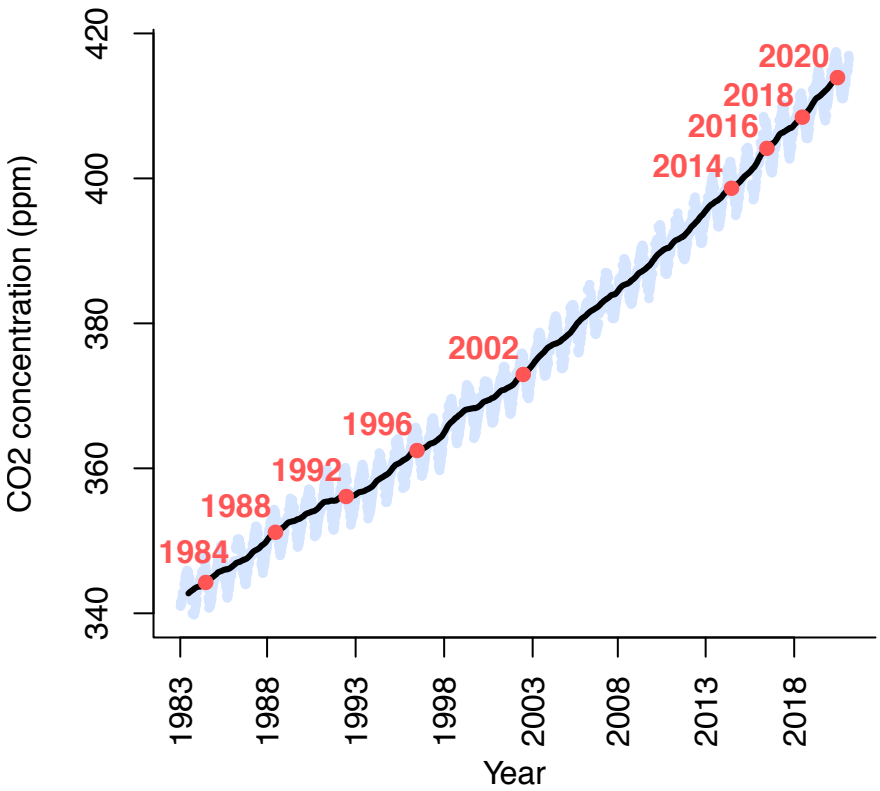

Fig. S2. **CO_2 concentration 1983 to 2021**. Data obtained from the Mauna Loa record, Scripps Institution of Oceanography, UC San Diego.

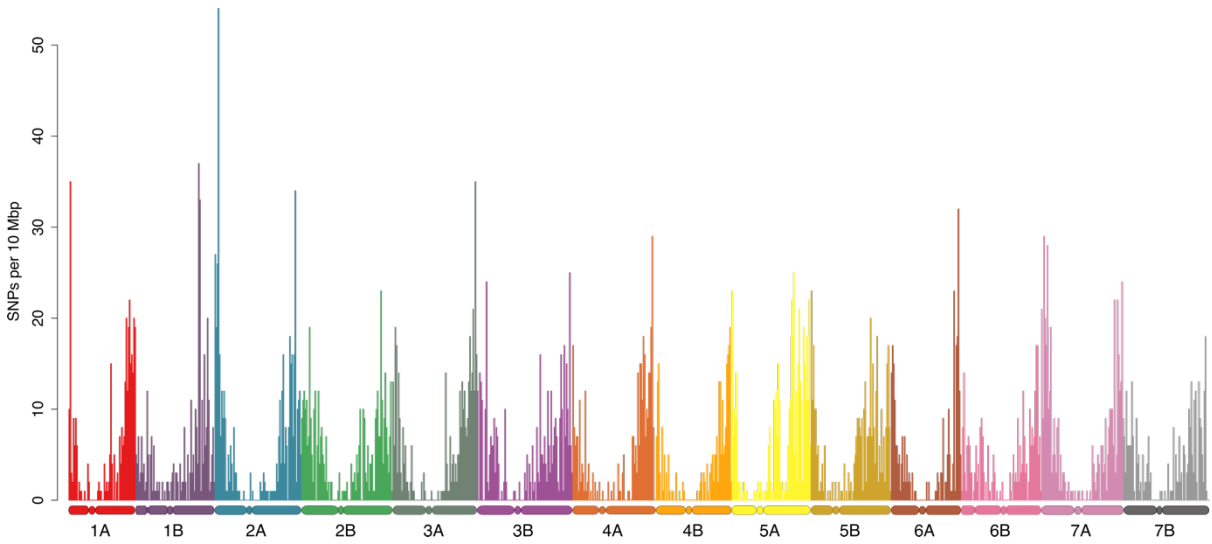

Fig. S3. **SNP density of 5196 markers along the wild emmer wheat genome.**

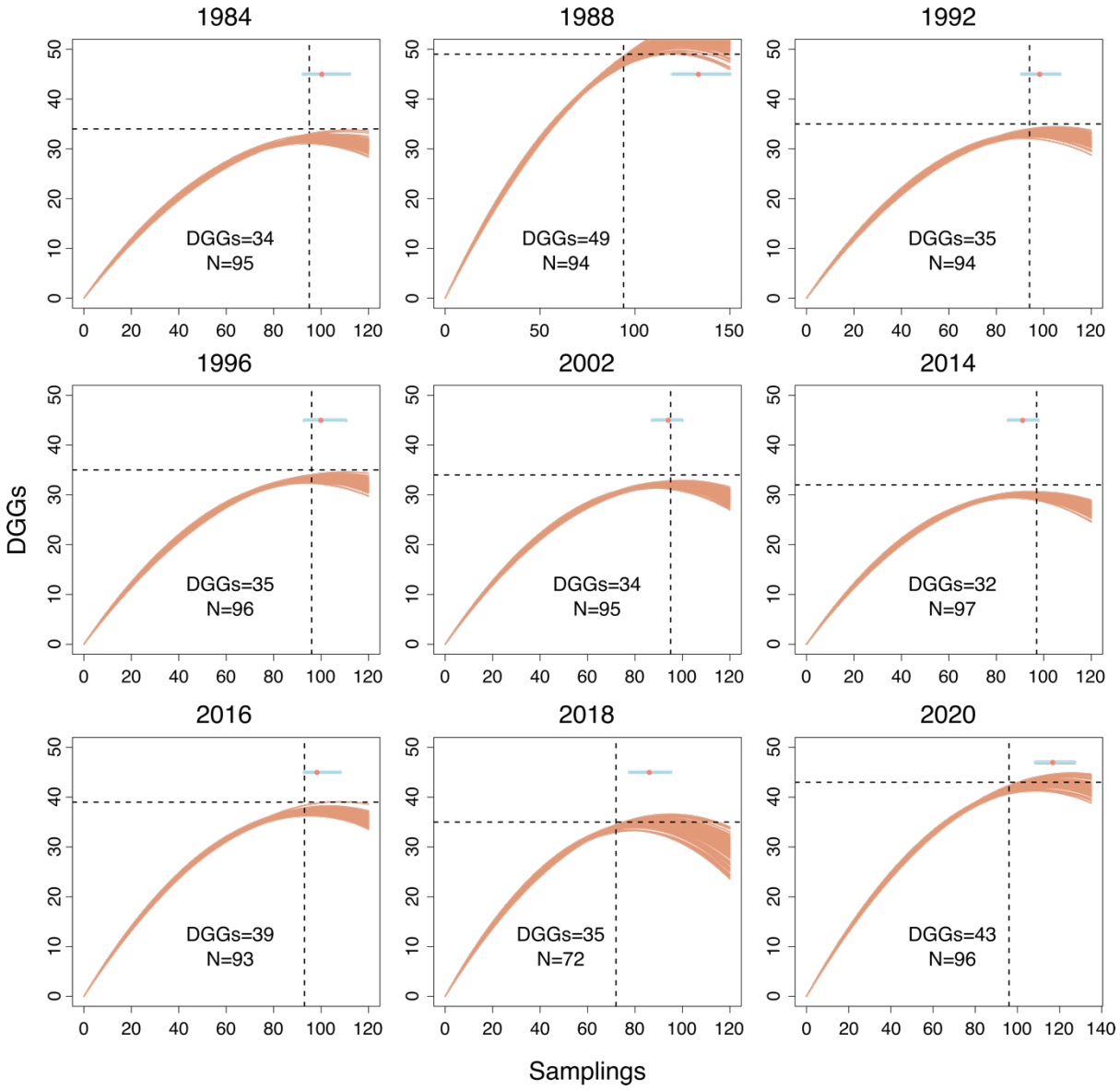

Fig. S4. **Rarefaction curves.** Adjusted 2nd degree polynomials of 100x backwards sample of unique genotype number and number of samples collected per year. Dashed horizontal line represents the observed number of unique genotypes per year, dashed vertical lines represent number of samples per year. Light blue line and red dot represent range and mean of inflection points over replicate subsamples respectively.

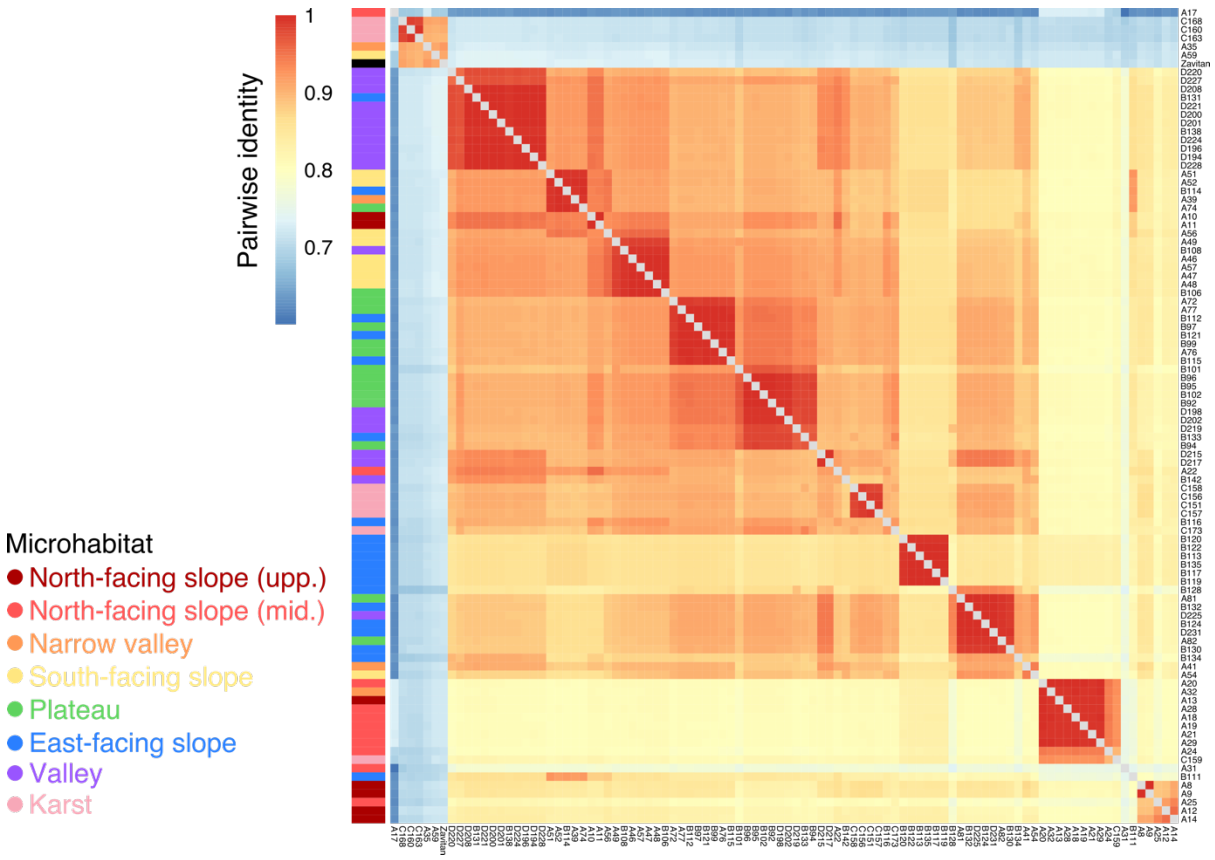

Fig. S5. **Population structure of Ammiad in the first year of collection (1984).** Heatmap colours represent identity value for each pairwise comparison, annotation colours (on the left) correspond to the list of microhabitats.

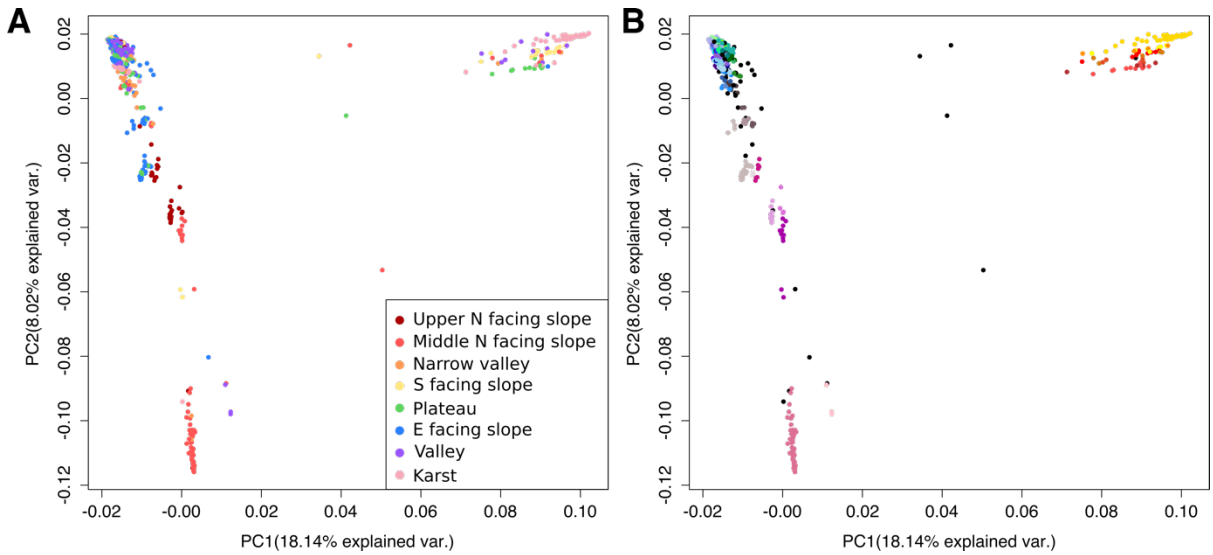

Fig. S6. **Principal Component Analysis of Ammiad collection.** (A) Coloured by microhabitat. (B) Coloured by DGGs, black dots represent singleton DGGs, which are not related to each other.

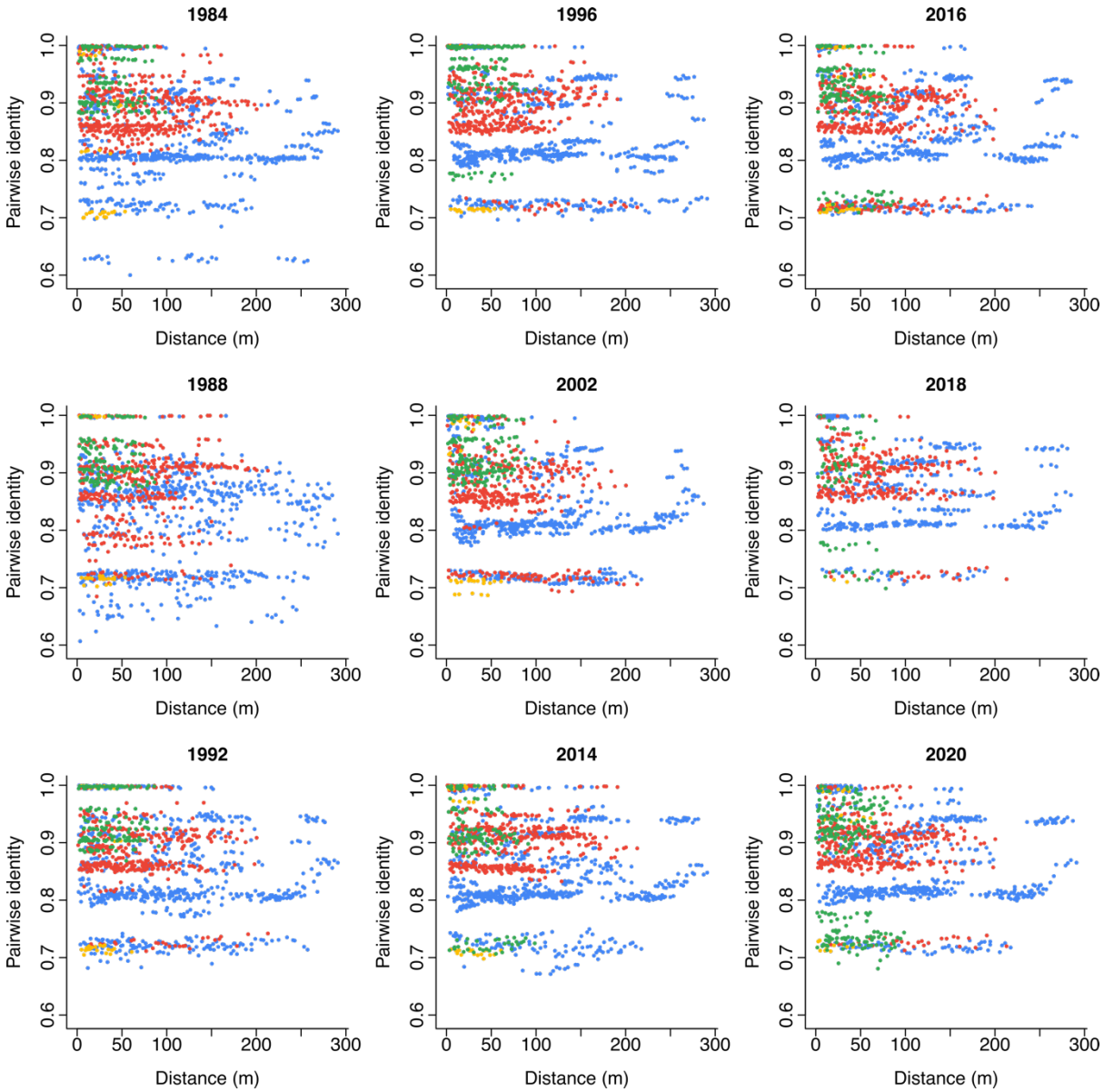

Fig. S7. **No evidence for isolation by distance in Ammiad collection.** Scatter plots of pairwise genetic identity and Euclidean distance (meters). Subplots show years of collection, and colours represent the different transects (A=blue, B=red, C=yellow, D=green).

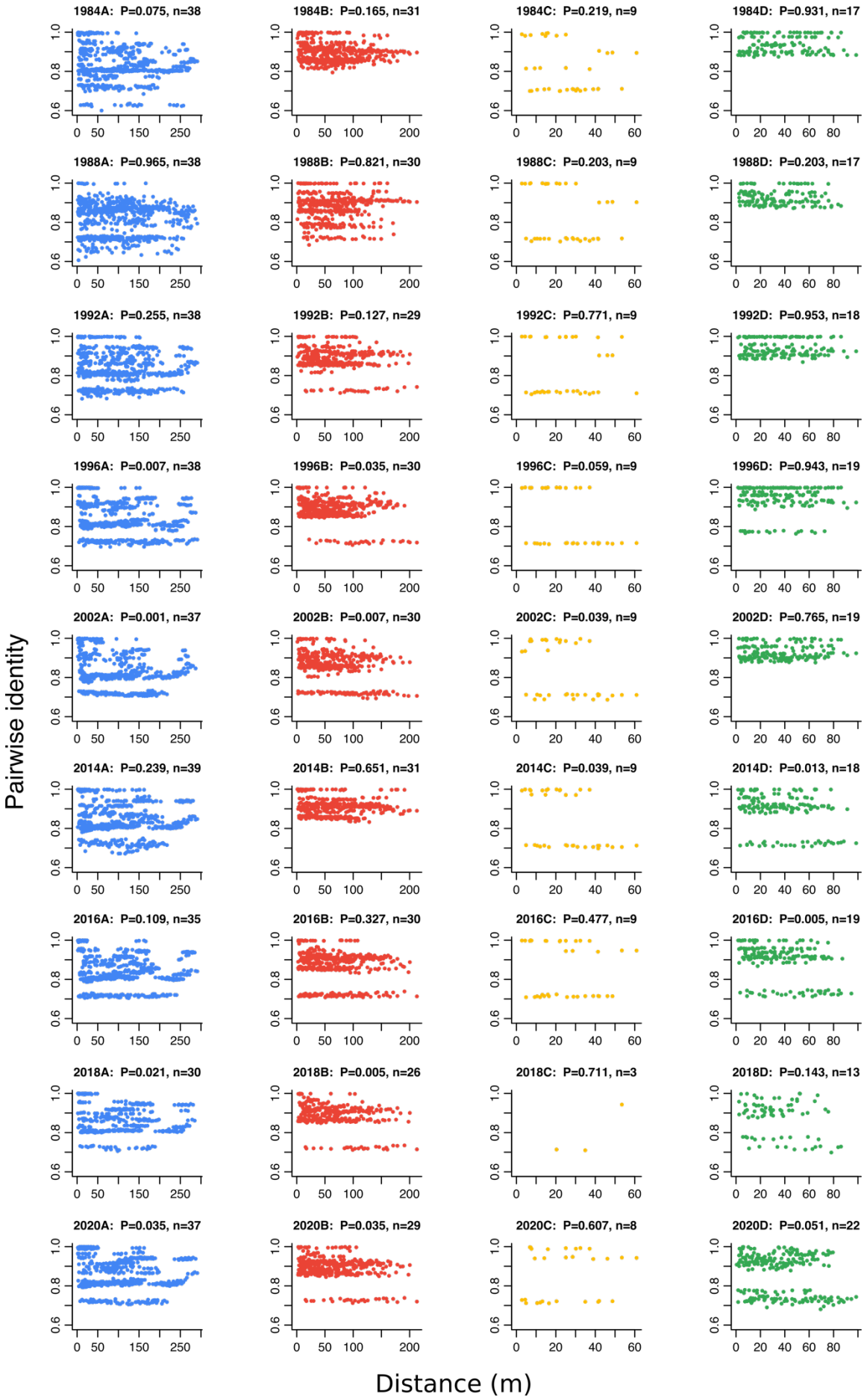
1984A: P=0.075, n=38
1984B: P=0.165, n=31
1984C: P=0.219, n=9
1984D: P=0.931, n=17
1988A: P=0.965, n=38
1988B: P=0.821, n=30
1988C: P=0.203, n=9
1988D: P=0.203, n=17
1992A: P=0.255, n=38
1992B: P=0.127, n=29
1992C: P=0.771, n=9
1992D: P=0.953, n=18
1996A: P=0.007, n=38
1996B: P=0.035, n=30
1996C: P=0.059, n=9
1996D: P=0.943, n=19
2002A: P=0.001, n=37
2002B: P=0.007, n=30
2002C: P=0.039, n=9
2002D: P=0.765, n=19
2014A: P=0.239, n=39
2014B: P=0.651, n=31
2014C: P=0.039, n=9
2014D: P=0.013, n=18
2016A: P=0.109, n=35
2016B: P=0.327, n=30
2016C: P=0.477, n=9
2016D: P=0.005, n=19
2018A: P=0.021, n=30
2018B: P=0.005, n=26
2018C: P=0.711, n=3
2018D: P=0.143, n=13
2020A: P=0.035, n=37
2020B: P=0.035, n=29
2020C: P=0.607, n=8
2020D: P=0.051, n=22
Pairwise identity
Distance (m)

Fig. S8. **Correlation and significance of isolation by distance in Ammiad collection.** Pairwise genetic identity by Euclidean distance (meters). Subplots show years of collection (rows) and transects (columns). The title of each plot indicates its number of samples and p-value from a Mantel test with 1000 permutations.

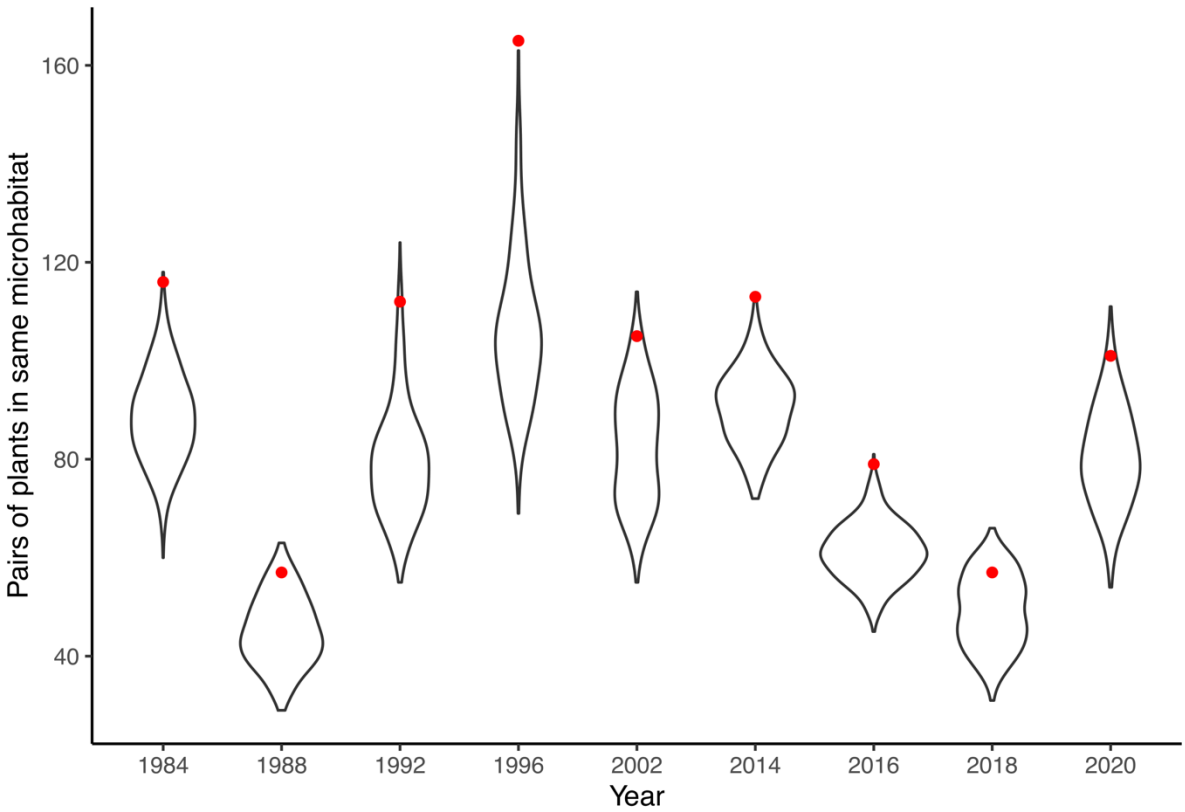

Fig. S9. **Sorting of plants of the same DGG by microhabitat comparing observed values (red) to values obtained by permuting habitat labels (violins).**

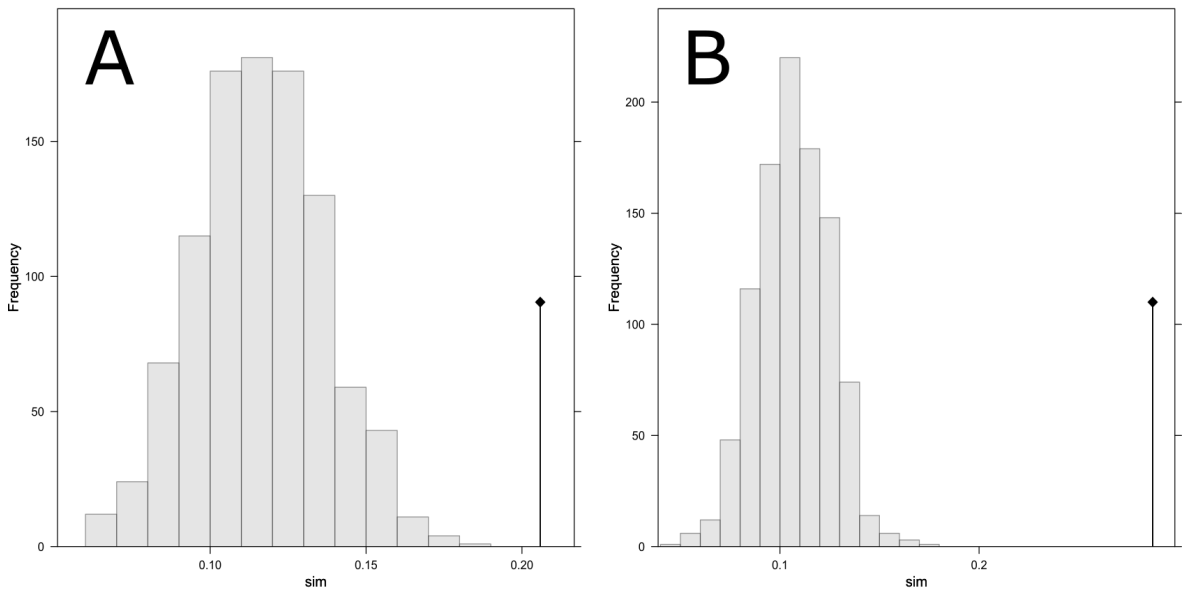

Fig. S10. **Histograms of 1000 spatially constrained randomizations of Mantel statistics (MSR-Mantel).** Observed values (black dots) versus randomizations for (A) pairwise genetic distances (p-value < 0.001) and (B) DGGs (p-value < 0.001).

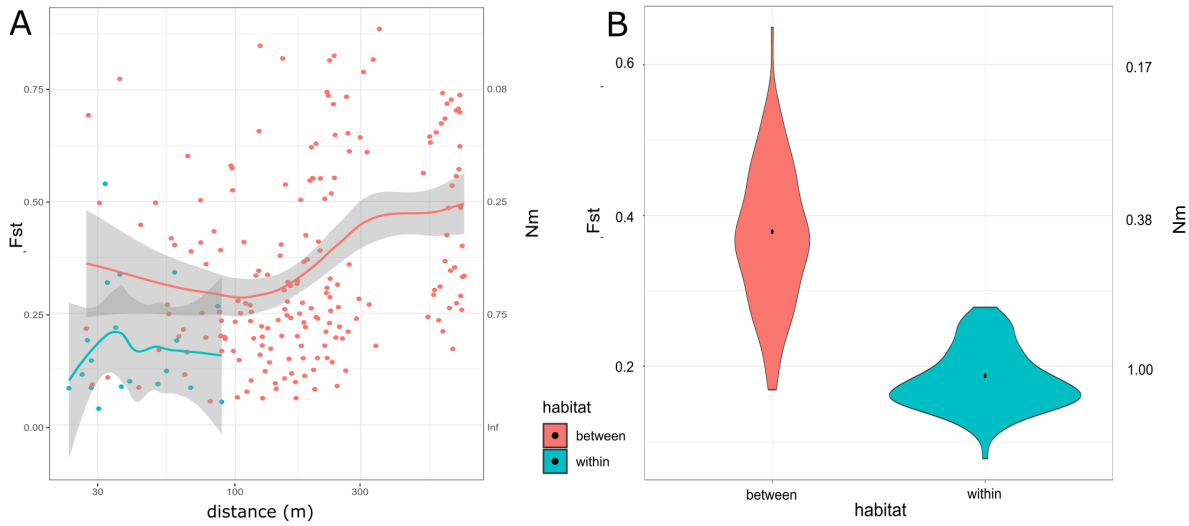

Fig. S11. **Genetic differentiation between and within habitats, accounting for spatial distance.** Plants within each habitat were grouped in 30m demes. Pairwise F_{st} was calculated among all demes, within and between habitats. A) Pairwise F_{st} plotted along distance, measured as the average distance of plants in the two demes. Credibility intervals of a loess fit with degree 1 are shown in grey. B) Pairwise F_{st} between demes with average distance <50m. Average observed values are shown as a black dot. Uncertainty was estimated with 1000 bootstraps of the parcels considered for the comparisons. Average within-habitat Fst was higher than between-habitat F_{st} in 3% of the bootstraps. For both A and B, Nm values (i.e. the theoretical number of migrants between parcels in an infinite island model) calculated are shown on the right axis.

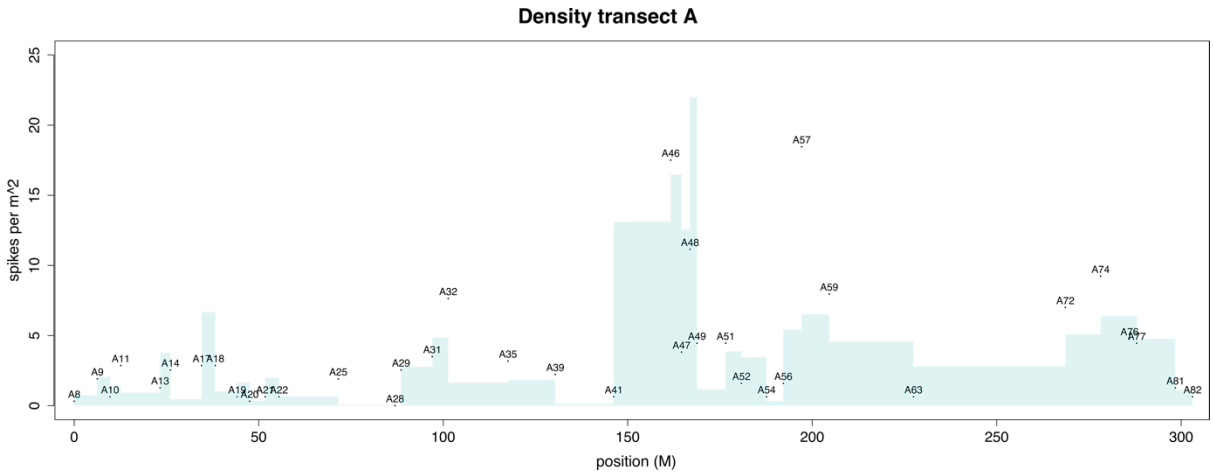

Fig. S12. **Spike density in transect A.** Spike density (corresponding to density of fertile plants) was measured around and between sampling sites (Table S4). Points represent the number of fertile spikes per 1 m^2 around the sampling point. Light blue bars represent normalized (to area) number of spikes from one sampling point to the following.

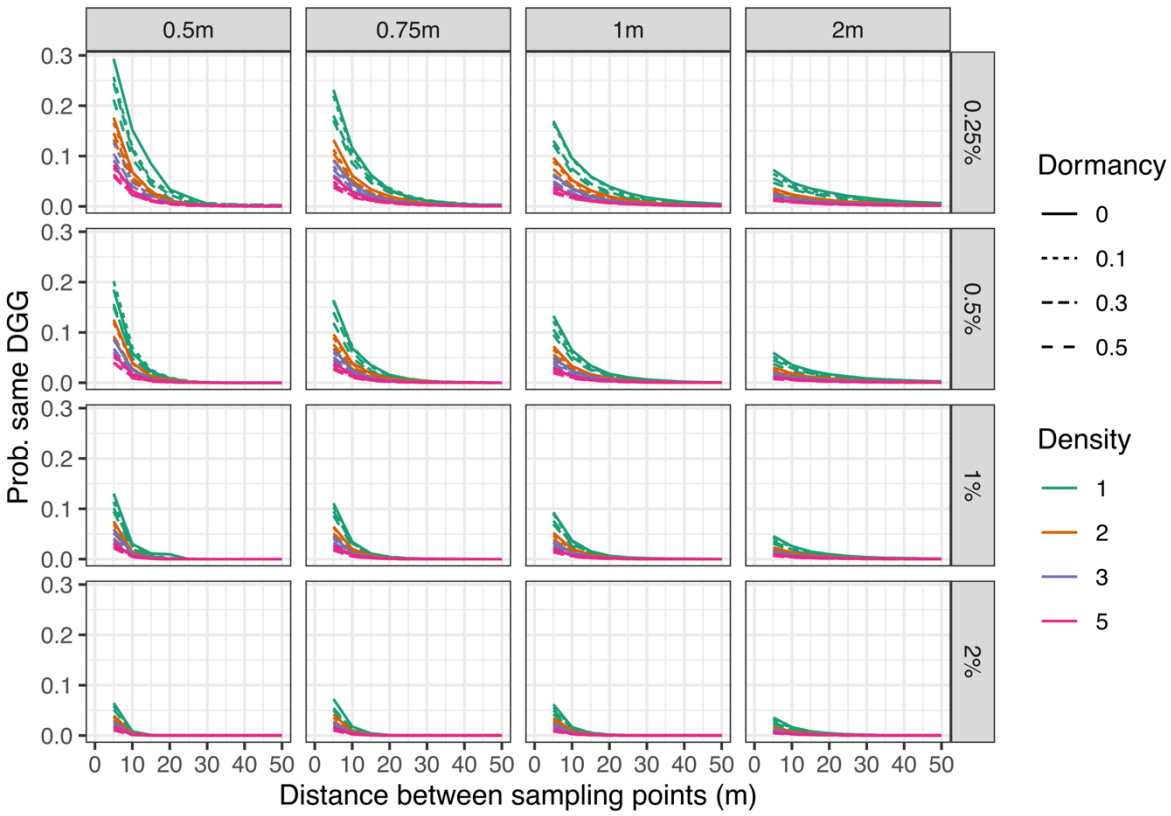

Fig. S13. **Spatial clustering along a transect in simulated populations.** Subplots show the probability of observing plants of the same DGG at pairs of sampling points at increasing distances, averaged over 100 replicate simulations. Panels indicate increasing mean seed dispersal distances (left to right) and increasing outcrossing rates (top to bottom). 'Dormancy' indicates the proportion of seeds drawn from the seed bank in each generation, and 'Density' the number of plants per square meter.

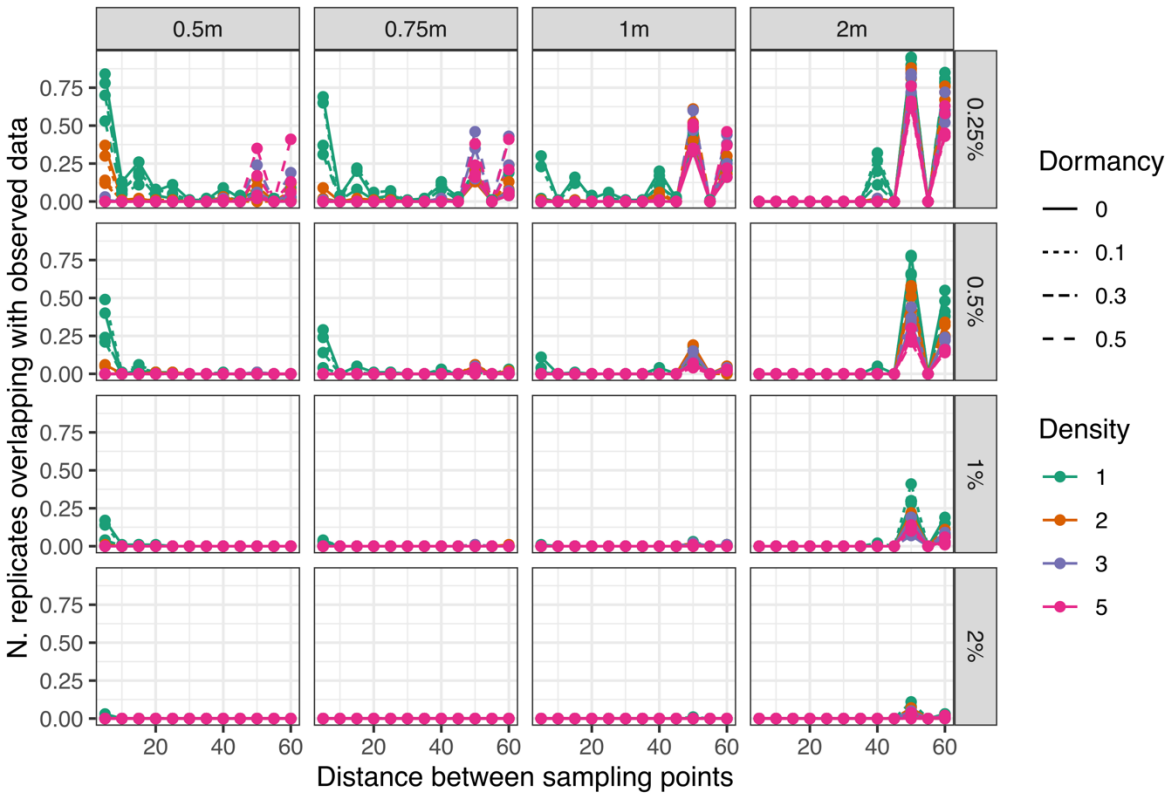

Fig. S14. **Overlap in spatial clustering between observed data and populations simulated under neutral demography.** Plots show the proportion of replicate simulations where pairs sampling points at different distances were more likely to be occupied by plants of the same DGG than in any observed transect. Panels indicate increasing mean seed dispersal distances (left to right) and increasing outcrossing rates (top to bottom). 'Dormancy' indicates the proportion of seeds drawn from the seed bank in each generation, and 'Density' the number of plants per square meter.

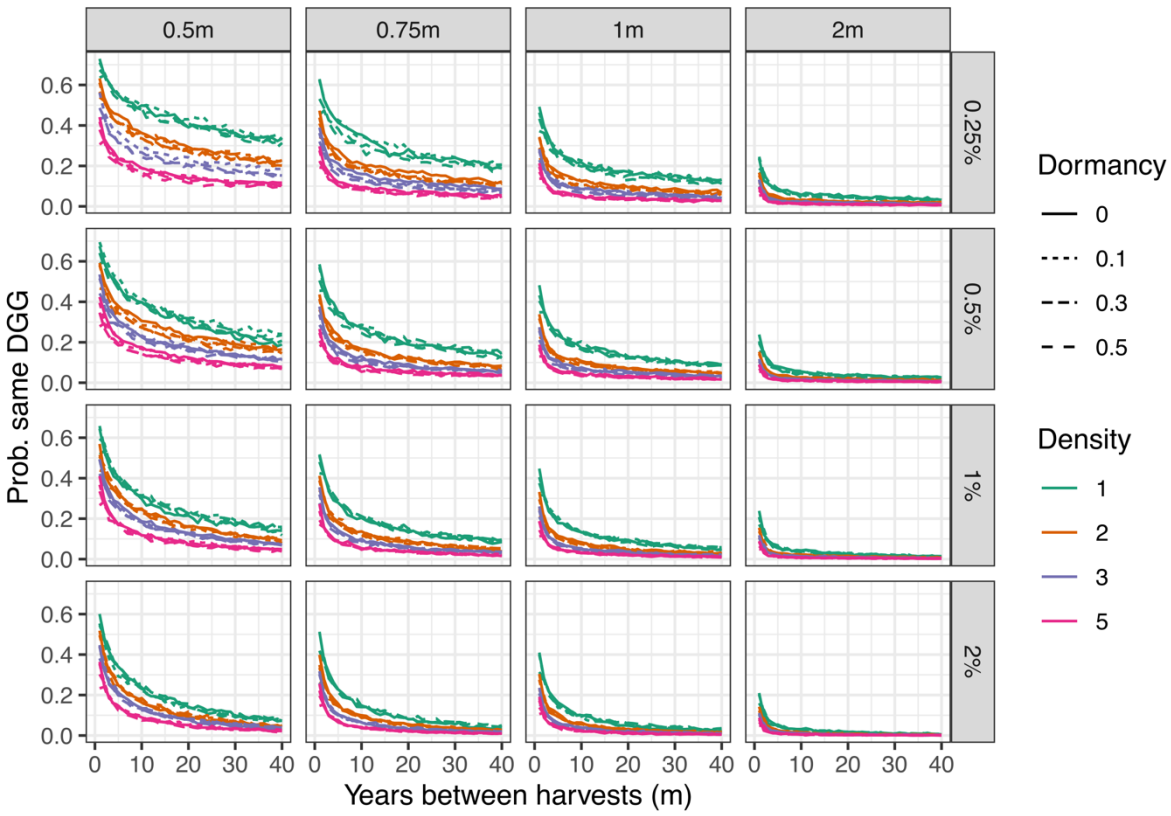

Fig. S15. **Temporal stability in simulated populations.** Subplots show the probability of observing plants of the same DGG at a single sampling in different years, averaged over 100 replicate simulations. Panels indicate increasing mean seed dispersal distances (left to right) and increasing outcrossing rates (top to bottom). 'Dormancy' indicates the proportion of seeds drawn from the seed bank in each generation, and 'density' the number of plants per square meter.

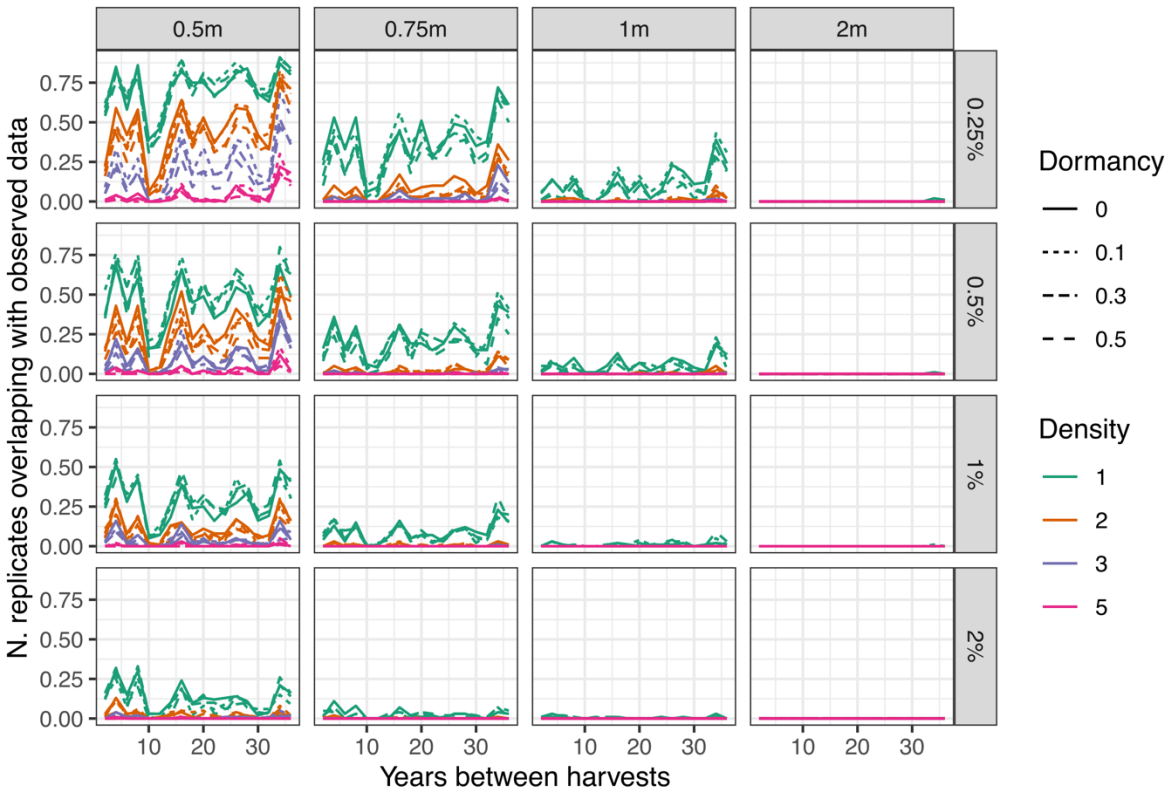

527

528 Fig. S16. **Probabilities that observed temporal stability could be generated by neutral**
529 **demography.** Plots show the proportion of replicate simulations where a single sampling point
530 sampled in different harvest years was more likely to be occupied by plants of the same DGG
531 than in any observed transect. Panels indicate increasing mean seed dispersal distances (left to
532 right) and increasing outcrossing rates (top to bottom). 'Dormancy' indicates the proportion of
533 seeds drawn from the seed bank in each generation, and 'Density' the number of plants per
534 square meter.

535

536

537

538

539

540

541

542 Table S1. **Ammiad sampling points coordinates.**

543

544 Table S2. **Dataset of Ammiad samples by genotype.**

545

546 Table S3. **Analysis of molecular variance of genotypes sampled in Ammiad across all**
547 **years, subdivided by habitat, using only polymorphic sites within Ammiad.** Sum of
548 squared deviations (SSD) and mean square deviations (MSD), variance components (**σ^2**) and
549 corresponding p-values were computed using the R package *pegas*. The Φ statistic for habitat
550 was used as an estimate of the proportion of molecular variance explained by the habitat
551 structure.

Component	**SSD**	**MSD**	**df**	**σ^2**	**p-value**	**Φ**
Habitat	0.9946	0.1421	7	0.0014	$<10^{-12}$	0.2833
Error	2.9429	0.0036	824	0.0036	/	/
Total	3.9374	0.0047	831	/	/	/

552

553 Table S4. **Spike density measured at transect A in 2020.**

554

555

556

557

558

559

560

561 **References**

562 Abebe TD, Naz AA, Léon J. 2015. Landscape genomics reveal signatures of local adaptation
563 in barley (Hordeum vulgare L.). *Front Plant Sci* **6**:813.
564 doi:10.3389/FPLS.2015.00813/BIBTEX
565 Anikster Y, Noy-Meir I. 1991. The wild-wheat field laboratory at Ammiad. *Isr J Bot* **40**:351–
566 362.
567 Avni R, Nave M, Barad O, Baruch K, Twardziok SO, Gundlach H, Hale I, Mascher M,
568 Spannagl M, Wiebe K, Jordan KW, Golan G, Deek J, Ben-Zvi B, Ben-Zvi G,
569 Himmelbach A, MacLachlan RP, Sharpe AG, Fritz A, Ben-David R, Budak H, Fahima
570 T, Korol A, Faris JD, Hernandez A, Mikel MA, Levy AA, Steffenson B, Maccaferri M,
571 Tuberosa R, Cattivelli L, Faccioli P, Ceriotti A, Kashkush K, Pourkheirandish M,
572 Komatsuda T, Eilam T, Sela H, Sharon A, Ohad N, Chamovitz DA, Mayer KFX, Stein
573 N, Ronen G, Peleg Z, Pozniak CJ, Akhunov ED, Distelfeld A. 2017. Wild emmer
574 genome architecture and diversity elucidate wheat evolution and domestication. *Science*
575 **357**:93–97. doi:10.1126/science.aan0032
576 Bradbury PJ, Zhang Z, Kroon DE, Casstevens TM, Ramdoss Y, Buckler ES. 2007. TASSEL:
577 software for association mapping of complex traits in diverse samples. *Bioinformatics*
578 **23**:2633–2635. doi:10.1093/bioinformatics/btm308
579 Consortium T 1001 G. 2016. 1,135 Genomes Reveal the Global Pattern of Polymorphism in
580 Arabidopsis thaliana. *Cell* **166**:481–491. doi:10.1016/J.CELL.2016.05.063
581 Crabot J, Clappe S, Dray S, Datry T. 2019. Testing the Mantel statistic with a spatially-
582 constrained permutation procedure. *Methods Ecol Evol* **10**:532–540. doi:10.1111/2041-
583 210X.13141
584 Danecek P, Auton A, Abecasis G, Albers CA, Banks E, DePristo MA, Handsaker RE, Lunter
585 G, Marth GT, Sherry ST, McVean G, Durbin R, Group 1000 Genomes Project Analysis.

586 2011. The variant call format and VCFtools. *Bioinformatics* **27**:2156–2158.
587 doi:10.1093/bioinformatics/btr330
588 Elshire RJ, Glaubitz JC, Sun Q, Poland JA, Kawamoto K, Buckler ES, Mitchell SE. 2011. A
589 Robust, Simple Genotyping-by-Sequencing (GBS) Approach for High Diversity
590 Species. *PLoS One* **6**:e19379. doi:10.1371/journal.pone.0019379
591 Felsenburg T, Levy AA, Galili G, Feldman M. 1991. Polymorphism of high-molecular-
592 weight glutenins in wild tetraploid wheat: spatial and temporal variation in a native site.
593 *Isr J Bot* **40**:451–479.
594 Frachon L, Libourel C, Villoutreix R, Carrère S, Glorieux C, Huard-Chauveau C, Navascués
595 M, Gay L, Vitalis R, Baron E, Amsellem L, Bouchez O, Vidal M, Le Corre V, Roby D,
596 Bergelson J, Roux F. 2017. Intermediate degrees of synergistic pleiotropy drive adaptive
597 evolution in ecological time. *Nat Ecol Evol 2017 110* **1**:1551–1561.
598 doi:10.1038/s41559-017-0297-1
599 Franks SJ, Sim S, Weis AE. 2007. Rapid evolution of flowering time by an annual plant in
600 response to a climate fluctuation. *Proc Natl Acad Sci* **104**:1278–1282.
601 doi:10.1073/PNAS.0608379104
602 Fu Y-B, Peterson GW, Horbach C, Konkin DJ, Beiles A, Nevo E. 2019. Elevated mutation
603 and selection in wild emmer wheat in response to 28 years of global warming. *Proc Natl*
604 *Acad Sci* **116**:20002–20008. doi:10.1073/PNAS.1909564116
605 Gardiner LJ, Joynson R, Omony J, Rusholme-Pilcher R, Olohan L, Lang D, Bai C,
606 Hawkesford M, Salt D, Spannagl M, Mayer KFX, Kenny J, Bevan M, Hall N, Hall A.
607 2018. Hidden variation in polyploid wheat drives local adaptation. *Genome Res*
608 **28**:1319–1332. doi:10.1101/GR.233551.117
609 Golenberg EM. 1988. Outcrossing rates and their relationship to phenology in Triticum
610 dicoccoides. *Theor Appl Genet* **75**:937–944. doi:10.1007/BF00258057

611 Golenberg EM. 1987. Estimation of gene flow and genetic neighborhood size by indirect
612 methods in a selfing annual, Triticum dicoccoides. *Evolution* **41**:1326–1334.
613 doi:10.1111/j.1558-5646.1987.tb02470.x
614 Hoffmann AA, Sgró CM. 2011. Climate change and evolutionary adaptation. *Nature*
615 **470**:479–485. doi:10.1038/nature09670
616 Horovitz A. 1998. The soil seed bank in wild emmerThe Proceedings of International
617 Symposium of In Situ Conservation of Plant Genetic Diversity. pp. 185–188.
618 Horovitz A, Feldman M. 1991. Evaluation of the wild-wheat study at Ammiad. *Isr J Bot*
619 **40**:501–508.
620 Keeling CD, Piper SC, Bacastow RB, Wahlen M, Whorf TP, Heimann M, Meijer HA. 2001.
621 Exchanges of Atmospheric CO2 and 13CO2 with the Terrestrial Biosphere and Oceans
622 from 1978 to 2000. I. Global Aspects. *I Glob Asp SIO Ref Ser* Scripps In:**88**.
623 Khoury CK, Carver D, Greene SL, Williams KA, Achicanoy HA, Schori M, León B,
624 Wiersema JH, Frances A. 2021. Crop wild relatives of the United States require urgent
625 conservation action. *Proc Natl Acad Sci U S A* **117**:33351–33357.
626 doi:10.1073/PNAS.2007029117
627 Legendre P, Fortin MJ, Borcard D. 2015. Should the Mantel test be used in spatial analysis?
628 *Methods Ecol Evol* **6**:1239–1247. doi:10.1111/2041-210X.12425
629 Levy AA, Feldman M. 1988. Ecogeographical distribution of HMW glutenin alleles in
630 populations of the wild tetraploid wheat Triticum turgidum var. dicoccoides. *Theor Appl*
631 *Genet* **75**:651–658. doi:10.1007/BF00289134
632 Li H. 2013. Aligning sequence reads, clone sequences and assembly contigs with BWA-
633 MEM. *arXiv*. doi:10.48550/arXiv.1303.3997
634 Li H, Handsaker B, Wysoker A, Fennell T, Ruan J, Homer N, Marth G, Abecasis G, Durbin
635 R, 1000 Genome Project Data Processing Subgroup. 2009. The Sequence

636 Alignment/Map format and SAMtools. *Bioinformatics* **25**:2078–2079.
637 doi:10.1093/bioinformatics/btp352
638 Nave M, Avni R, Çakır E, Portnoy V, Sela H, Pourkheirandish M, Ozkan H, Hale I,
639 Komatsuda T, Dvorak J, Distelfeld A. 2019. Wheat domestication in light of haplotype
640 analyses of the Brittle rachis 1 genes (BTR1-A and BTR1-B). *Plant Sci* **285**:193–199.
641 doi:10.1016/j.plantsci.2019.05.012
642 Nevo E. 2009. Evolution in action across life at "Evolution Canyons", Israel. *Trends Evol*
643 *Biol* **1**:e3–e3. doi:10.4081/EB.2009.E3
644 Noy-Meir I, Agami M, Anikster Y. 1991a. Changes in the population density of wild emmer
645 wheat (Triticum turgidum var. dicoccoides) in a mediterranean grassland. *Isr J Bot*
646 **40**:385–395.
647 Noy-Meir I, Agami M, Cohen E, Anikster Y. 1991b. Floristic and ecological differentiation
648 of habitats within a wild wheat population at Ammiad. *Isr J Bot* **40**:363–384.
649 Ozbek O, Millet E, Anikster Y, Arslan O, Feldman M. 2007. Spatio-temporal genetic
650 variation in populations of wild emmer wheat, Triticum turgidum ssp. dicoccoides, as
651 revealed by AFLP analysis. *Theor Appl Genet 2007 1151* **115**:19–26.
652 doi:10.1007/S00122-007-0536-Y
653 Paradis E. 2010. pegas: an R package for population genetics with an integrated-modular
654 approach. *Bioinformatics* **26**:419–420. doi:10.1093/BIOINFORMATICS/BTP696
655 Paradis E, Claude J, Strimmer K. 2004. APE: Analyses of phylogenetics and evolution in R
656 language. *Bioinformatics* **20**:289–290. doi:10.1093/bioinformatics/btg412
657 Pecl GT, Araújo MB, Bell JD, Blanchard J, Bonebrake TC, Chen IC, Clark TD, Colwell RK,
658 Danielsen F, Evengård B, Falconi L, Ferrier S, Frusher S, Garcia RA, Griffis RB,
659 Hobday AJ, Janion-Scheepers C, Jarzyna MA, Jennings S, Lenoir J, Linnetved HI,
660 Martin VY, McCormack PC, McDonald J, Mitchell NJ, Mustonen T, Pandolfi JM,

661 Pettorelli N, Popova E, Robinson SA, Scheffers BR, Shaw JD, Sorte CJB, Strugnell JM,
662 Sunday JM, Tuanmu MN, Vergés A, Villanueva C, Wernberg T, Wapstra E, Williams
663 SE. 2017. Biodiversity redistribution under climate change: Impacts on ecosystems and
664 human well-being. *Science* **355**. doi:10.1126/science.aai9214
665 Poland JA, Brown PJ, Sorrells ME, Jannink J-L. 2012. Development of High-Density
666 Genetic Maps for Barley and Wheat Using a Novel Two-Enzyme Genotyping-by-
667 Sequencing Approach. *PLoS One* **7**:e32253. doi:10.1371/journal.pone.0032253
668 Poplin R, Ruano-Rubio V, DePristo MA, Fennell TJ, Carneiro MO, Auwera GA Van der,
669 Kling DE, Gauthier LD, Levy-Moonshine A, Roazen D, Shakir K, Thibault J, Chandran
670 S, Whelan C, Lek M, Gabriel S, Daly MJ, Neale B, MacArthur DG, Banks E. 2018.
671 Scaling accurate genetic variant discovery to tens of thousands of samples. *bioRxiv*
672 201178. doi:10.1101/201178
673 Salamini F, Özkan H, Brandolini A, Schäfer-Pregl R, Martin W. 2002. Genetics and
674 geography of wild cereal domestication in the near east. *Nat Rev Genet* **3**:429–441.
675 doi:10.1038/nrg817
676 Schemske DW. 1984. Population structure and local selection in Impatiens pallida
677 (balsaminaceae), a selfing annual. *Evolution* **38**:817–832.
678 Sedlacek J, Cortés AJ, Wheeler J, Bossdorf O, Hoch G, Klápště J, Lexer C, Rixen C, Wipf S,
679 Karrenberg S, van Kleunen M. 2016. Evolutionary potential in the Alpine: trait
680 heritabilities and performance variation of the dwarf willow Salix herbacea from
681 different elevations and microhabitats. *Ecol Evol* **6**:3940–3952. doi:10.1002/ECE3.2171
682 Siepielski AM, Dibattista JD, Carlson SM. 2009. It's about time: The temporal dynamics of
683 phenotypic selection in the wild. *Ecol Lett* **12**:1261–1276. doi:10.1111/J.1461-
684 0248.2009.01381.X
685 Snir A, Nadel D, Groman-Yaroslavski I, Melamed Y, Sternberg M, Bar-Yosef O, Weiss E.

686 2015. The Origin of Cultivation and Proto-Weeds, Long Before Neolithic Farming.
687 *PLoS One* **10**:e0131422. doi:10.1371/JOURNAL.PONE.0131422
688 Urban MC. 2015. Accelerating extinction risk from climate change. *Science* **348**:571–573.
689 doi:10.1126/science.aaa4984
690 Volis S, Anikster Y, Olsvig-Whittaker L, Mendlinger S. 2004. The influence of space in
691 genetic-environmental relationships when environmental heterogeneity and seed
692 dispersal occur at similar scale. *Am Nat* **163**:312–327. doi:10.1086/381406
693 Volis S, Ormanbekova D, Shulgina I. 2016. Fine-scale spatial genetic structure in
694 predominantly selfing plants with limited seed dispersal: A rule or exception? *Plant*
695 *Divers* **38**:59–64. doi:10.1016/J.PLD.2016.03.001
696 Volis S, Ormanbekova D, Yermekbayev K, Song M, Shulgina I. 2015. Multi-Approaches
697 Analysis Reveals Local Adaptation in the Emmer Wheat (Triticum dicoccoides) at
698 Macro- but not Micro-Geographical Scale. *PLoS One* **10**:e0121153.
699 doi:10.1371/JOURNAL.PONE.0121153
700 Wintle BA, Kujala H, Whitehead A, Cameron A, Veloz S, Kukkala A, Moilanen A, Gordon
701 A, Lentini PE, Cadenhead NCR, Bekessy SA. 2019. Global synthesis of conservation
702 studies reveals the importance of small habitat patches for biodiversity. *Proc Natl Acad*
703 *Sci U S A* **116**:909–914. doi:10.1073/pnas.1813051115
704 Zeder MA. 2011. The origins of agriculture in the Near East. *Curr Anthropol* **52**.
705 doi:10.1086/659307/0
706 Zheng X, Levine D, Shen J, Gogarten SM, Laurie C, Weir BS. 2012. A high-performance
707 computing toolset for relatedness and principal component analysis of SNP data.
708 *Bioinformatics* **28**:3326. doi:10.1093/BIOINFORMATICS/BTS606
709 Zhu T, Wang L, Rodriguez JC, Deal KR, Avni R, Distelfeld A, McGuire PE, Dvorak J, Luo
710 M-C. 2019. Improved Genome Sequence of Wild Emmer Wheat Zavitan with the Aid of

711 Optical Maps. *G3 (Bethesda)* **9**:619–624. doi:10.1534/g3.118.200902

712 Zsögön A, Peres LEP, Xiao Y, Yan J, Fernie AR. 2021. Enhancing crop diversity for food

713 security in the face of climate uncertainty. *Plant J* **109**:402–414. doi:10.1111/TPJ.15626

714